ISBN: 978-3-95450-227-1 ISSN: 2673-5490 doi:10.18429/JACoW-IPAC2022-WEPOST043

AN EFFECTIVE-DENSITY MODEL FOR ACCELERATING FIELDS IN LASER-GRAPHENE INTERACTIONS

C. Bonţoiu*, Ö. Apsimon[1], E. Kukstas, C. Welsch[1], M. Yadav
University of Liverpool, Liverpool, UK
G. Xia[1], University of Manchester, MManchester, UK
J. Resta-López, University de Valencia, Valencia, Spain
A. Bonatto, Federal University of Health Sciences of Porto Alegre, Brazil
[1]also at Cockroft Institute, Daresbury, UK

Abstract

With the advancement of high-power UV laser technology, the use of nanostructures for particle acceleration attracts renewed interest due to its possibility of achieving TV/m accelerating gradients in solid state plasmas. Electron acceleration in ionized materials such as carbon nanotubes and graphene is currently considered as a potential alternative to the usual laser wakefield acceleration (LWFA) schemes. An evaluation of the suitability of a graphene target for LWFA can be carried out using an effective density model, thus replacing the need to model each layer. We present a 2D evaluation of the longitudinal electric field driven by a short UV laser pulse in a multi-layer graphene structure, showing that longitudinal fields of ~5 TV/m are achievable.

INTRODUCTION

Unlike LWFA in gases, which can be achieved with laser pulses in the IR range, at peak intensities of 10^{18}-10^{19} W/cm^2 [1], the equivalent mechanism in solid-state plasmas requires an UV laser pulse with peak intensity in the range 10^{20}-10^{21} W/cm^2, because charge densities in solids are 4–5 orders of magnitude higher than in gas targets. Graphene [2] can be grown in the form of 2D layers of Carbon atoms, stacked together with a controllable inter-layer gap of a few nm. Due to its unique optical [3] and electronic [4] properties graphene is used as a medium for applications such as high-harmonic generation [5] or terahertz radiation [6]. Moreover, when fully ionized by intense laser pulses, each graphene layer delivers plasma with an electron density of $\sim 10^{23}$ cm^{-3} and the tunability of the inter-layer gap implies that variable effective plasma densities of $\sim 10^{22}$ cm^{-3} can be obtained. This enables resonant propagation of sufficiently intense laser pulses with wavelengths of up to 300 nm, and also allows electrons to move easier along the inter-layer gaps. Realistic Particle-In-Cell (PIC) simulations rely the capability of using mesh cells a few times smaller than the layer thickness, 0.34 nm and this poses a significant numerical overhead. However, reasonably accurate estimates of the electric fields can be obtained using an *effective density* equivalent. However, one should note that this approximation prevents the possibility to realistically study transient plasma dynamics at a resolution smaller than the inter-layer gap. To build it from a *layered target* model, the total amount of unperturbed charge is kept constant and uniformly distributed in the bulk volume of the target. The concept of effective density was already applied for PIC simulations involving electron bunches colliding with carbon nanotubes [7]. We have used the PIConGPU code [8] to evaluate the dynamics and magnitude of the longitudinal electric field in laser-graphene interactions.

SIMULATION SETUP

The 2D model uses a 1.2 µm-wide and 1.5 µm-long target, as the *effective density* equivalent of 60 graphene layers, spaced by 20 nm-wide edge-to-edge gaps. The laser pulse is Gaussian, both transversely with an FWHM spot size 400 nm, and longitudinally with 1 fs FWHM pulse duration. It has a linear polarization within the $yx-$plane. The carbon plasma *effective density* is initialized as $n_0 = 1.94 \times 10^{21}$ cm^{-3} but rises to $6\,n_0 = 1.61 \times 10^{22}$ cm^{-3} as the target is virtually instantaneously ionized completely. The mesh cell size is limited to 0.25 nm with 1 macroparticle per mesh cell. Moving rightwards along the $y-$axis (longitudinal), the laser pulse interacts with the target for 16 fs which corresponds to 48 cycles, and travels 4.8 µm. Table 1 lists all important laser parameters. The simulation ignores lattice effects since the carbon atoms are generated uniformly across the target volume and there is no ionization threshold specific to graphene. Three ionization mechanisms (barrier suppression, tunneling and collisional) are enabled but they use atom ionization levels. Recombination is not considered but it can be ignored, given the short interaction time studied in this work (10 fs). For the same reason, the motion of the carbon ions, evaluated at a few nm, does not affect the overall results.

Table 1: Laser Parameters

Quantity	Value	Unit
wavelength: λ	100	nm
period: T_{laser}	0.334	fs
peak intensity: I_0	10^{21}	W/cm^2
spot size*: w_0	0.4	µm
focal point: y_0	0.25	µm
pulse energy: ΔE	8	mJ
pulse length§: Δt	3	fs

*FWHM, §9 cycles

* Cristian.Bontoiu@liverpool.ac.uk

ISBN: 978-3-95450-227-1 ISSN: 2673-5490 doi:10.18429/JACoW-IPAC2022-WEPOST043

THE ELECTRIC FIELD

As the carbon atoms are continuously ionized, electrons are expelled alternatively towards the upper/lower transverse edges of the target and drift backwards towards lower $y-$coordinates. These electrons also tend to neutralize the carbon ions behind the laser pulse, gathering towards the longitudinal axis of the target, $x = 0.8\,\mu$m. A bubble region is thus formed in the trail of the laser pulse. The first half of the bubble contains C^{6+} ions with a dense sheet of electrons to the right, yielding a positive longitudinal electric field, while for the second half of the bubble this is placed to the left resulting in a negative electric field. This situation is shown in Fig. 1, where the local minimum and maximum of the longitudinal field are also marked within the first bubble.

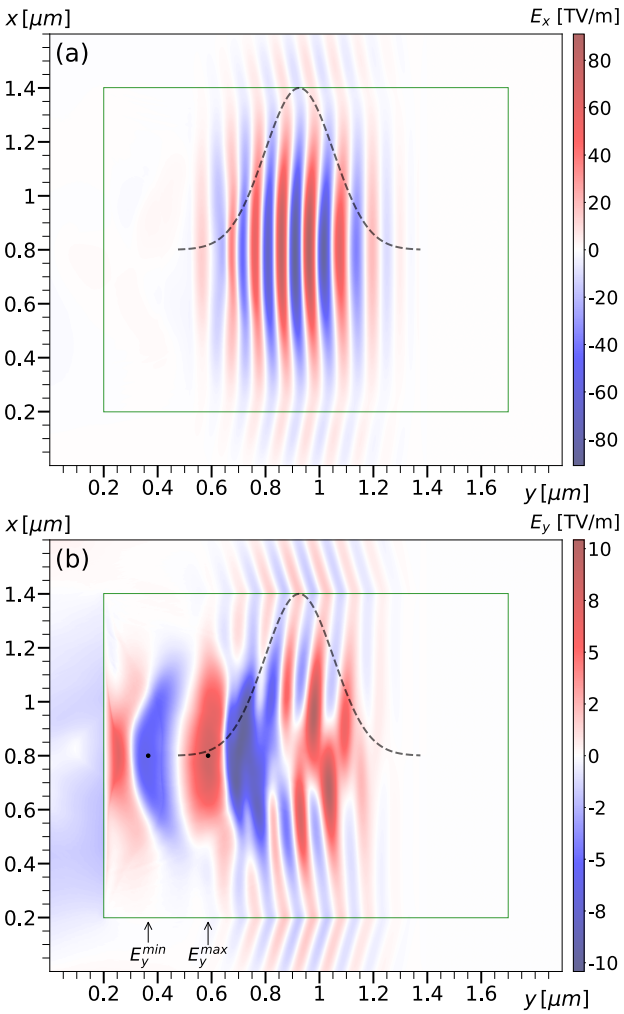

Figure 1: (a) Transverse and (b) longitudinal electric field, driven by the laser pulse at $t/T_{laser} \sim 14$. The unperturbed target boundaries are shown by the green rectangle and the two dots respectively indicate a local minimum and maximum of E_y, in the trail of the laser pulse, shown by the dashed black line.

Electrons injected in the left half of the bubble by external means (i.e. from a photocathode) or collected from the plasma can be accelerated by using the relatively stable $4-6$ TV/m longitudinal gradient. Stability here means the persistence of only two compact regions of longitudinal electric field: a positive one and a negative one. The curvature of the $E_y = 0$ contours increases gradually due to different phase velocities across the target width (x, transverse direction) which originates from the Gaussian transverse profile of the laser pulse. Thus, the bubbles deform and have a tendency to split into halves. Such a situation is shown in Fig. 2. Recording the evolution of the local minimum in the

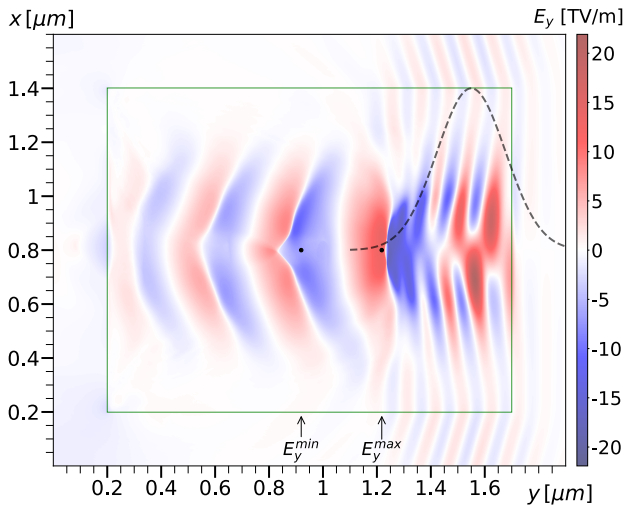

Figure 2: Longitudinal electric field, driven by the laser pulse at $t/T_{laser} \sim 20$. From this moment the first bubble cannot be sustained by the laser pulse and gradually vanishes.

first bubble is important as an estimate of the available field. As shown in Fig. 3 the local maximum and minimum are not equal in absolute value, but both grow linearly, as long as ionization is ongoing, either by direct laser ionization or collisional ionization. The first bubble appears at $t/T_{laser} \sim 14$ and propagates intact up to $t/T_{laser} \sim 21$. It is then gradually destroyed due to laser depletion and, as a consequence, there is a sharp decrease of the local maximum and minimum of E_y. While falling off, the time lag between the two extreme points is $\sim 2.5\,T_{laser}$. The electric field configuration favourable to acceleration lasts for 7 laser cycles due to the significant depletion of the laser pulse. This is shown in Fig. 4 where E_y and E_x are shown at two distinct times. The insets show the on-axis electric fields inside the first bubble behind the laser pulse.

CONCLUSION

In this study we have shown that TV/m electric fields are achievable in solid state plasmas based on multilayer graphene, in the form of stable longitudinal bubbles ~0.3 μm-long. The bubbles propagate for ~1 μm and their negative phase may be used to accelerate electrons. This

ISBN: 978-3-95450-227-1 ISSN: 2673-5490 doi:10.18429/JACoW-IPAC2022-WEPOST043

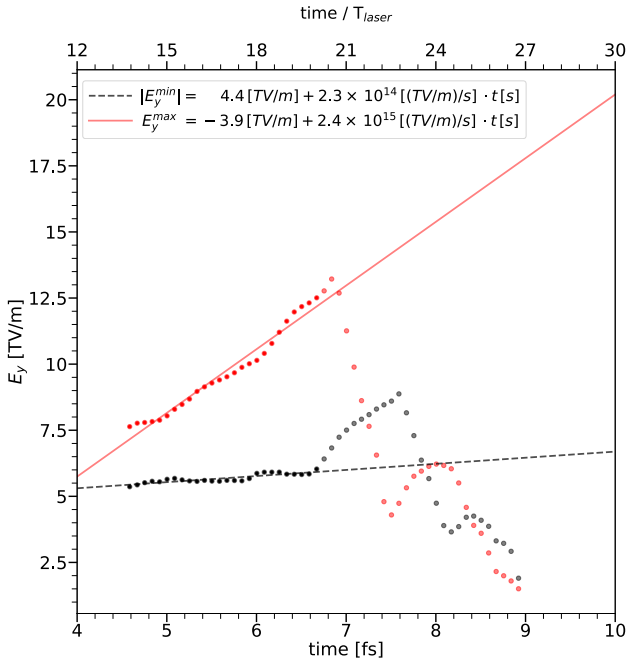

Figure 3: Maximum positive (red) and minimum negative (black, in absolute value) longitudinal electric field in the first bubble.

work supports alternative routes to the design of high-gradient compact accelerators, using solid-state plasmas.

ACKNOWLEDGEMENTS

We acknowledge the technical support received from the PIConGPU [8] software developers and the required computational infrastructure provided by the University of Liverpool LivDAT Framework [9]. J. Resta-López acknowledges support by the Generalitat Valencia under grant agreement CIDEGENT / 2019 / 058.

REFERENCES

[1] E. Esarey, C. Schroeder, W. Leemans, "Physics of laser-driven plasma-based electron accelerators", *Rev. Mod. Phys.*, vol. 81, pp. 1229–1285, 2009.

[2] M. Katsnelson, "The Physics of Graphene", Cambridge University Press, 2020.

[3] R. Binder, "Optical Properties of Graphene", World Scientific, 2016.

[4] A. Neto, F. Guinea, N. Peres, K. Novoselov, A. Geim, "The electronic properties of graphene", *Rev. Mod. Phys.*, vol. 81, pp. 109–162, 2009.

[5] M. Mrudul, G. Dixit, "High-harmonic generation from monolayer and bilayer graphene", *Phys. Rev. B.*, vol. 103, p. 094308, 2021.

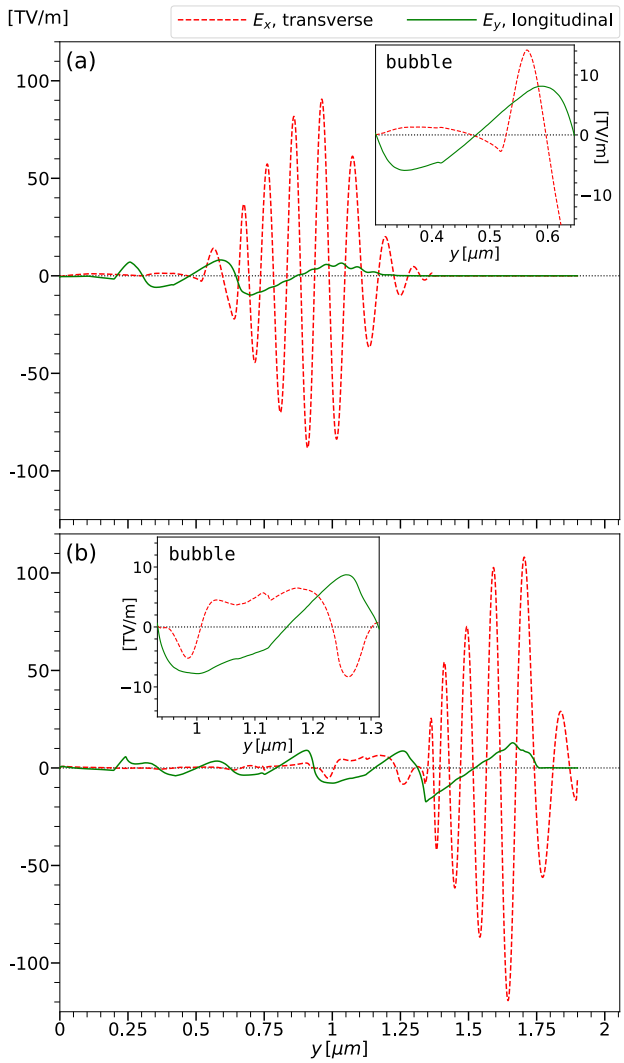

Figure 4: Transverse (dashed, red) and longitudinal (solid, green) on-axis electric fields shown: (a) at t/T_{laser} ~14 when the first bubble appears and (b) at t/T_{laser} ~21 when the destruction of first bubble starts.

[6] K. Batrakov, S. Maksimenko, "Graphene layered systems as a terahertz source with tuned frequency", *Phys. Rev. B.*, vol. 95, p. 205408, 2017.

[7] A. Bonatto *et al.*, "Exploring ultra-high-intensity wakefields in carbon nanotube arrays: an effective plasma-density approach", in preparation.

[8] H. Burau *et al.*, "PIConGPU: A Fully Relativistic Particle-in-Cell Code for a GPU Cluster", *IEEE Trans. Plasma Sci.*, vol. 38, pp. 2831–2839, 2010.

[9] Liverpool Big Data Science Centre for Doctoral Training, www.liverpool.ac.uk/livdat